

1 **Polar front shift and atmospheric CO₂ during the glacial maximum of the Early**

2 **Paleozoic Icehouse**

3
4 Thijs R. A. Vandenbroucke^{1,2,3*}, Howard A. Armstrong¹, Mark Williams^{4,5}, Florentin
5 Paris⁶, Jan A. Zalasiewicz⁴, Koen Sabbe⁷, Jaak Nõlvak⁸, Thomas J. Challands^{1,9},
6 Jacques Verniers² and Thomas Servais³

7
8 ¹*Palaeoclimate Group, Department of Earth Sciences, Durham University, Science Labs, Durham, DH1 3LE, UK*

9 ²*Research Unit Palaeontology, Department of Geology, Ghent University, Krijgslaan 281-S8, 9000 Ghent,*
10 *Belgium*

11 ³*Géosystèmes, Université Lille 1, FRE 3298 du CNRS, Avenue Paul Langevin, bâtiment SN5, 59655 Villeneuve*
12 *d'Ascq cedex, France*

13 ⁴*Department of Geology, University of Leicester, University Road, Leicester, LE1 7RH, UK*

14 ⁵*British Geological Survey, Kingsley Dunham Centre, Keyworth, NG12 5GG, UK*

15 ⁶*Géosciences, Université de Rennes I, UMR 6118 du CNRS, Campus de Beaulieu, 35042 Rennes-cedex, France*

16 ⁷*Protistology and Aquatic Ecology, Department of Biology, Ghent University, Krijgslaan 281-S8, 9000 Ghent,*
17 *Belgium*

18 ⁸*Institute of Geology, Tallinn University of Technology, Ehitajate tee 5, 19086 Tallinn, Estonia*

19 ⁹*Total E&P UK Limited, Geoscience Research Centre, Crawpeel Road, Aberdeen AB12 3FG, UK*

20
21 * corresponding author: Current address, see 3.
22 E-mail: Thijs.vandenbroucke@univ-lille1.fr
23 Tel. + 33 (0)3 20 43 69 00
24

25 **Author Contributions**

26 TVDB, HAA and MW contributed equally: they designed the project together with JAZ, conceived the
27 concept, interpreted the data and wrote the paper. TVDB assembled the data. FP, JN and TJC provided
28 chitinozoan distribution data. KS established the biostatistical protocol and performed the analysis. JV
29 and TS supervised the project. All authors discussed the results and implications and commented on the
30 manuscript.

31

32 **Competing Financial Interests statement**

33 The authors declare no competing (financial) interests.

34

35 **Classification:** Physical Sciences: Geology.

36

37 **Supplementary information** accompanies this paper:

38 Materials and Methods

39 Results

40 Literature sources for Late Ordovician *p*CO₂ estimates

41 Figs. S1, S2, S3, S4.

42

43 **Our new data address the paradox of Late Ordovician glaciation under**
44 **supposedly high $p\text{CO}_2$ (8 to 22x PAL: Pre-industrial Atmospheric Level). The**
45 **paleobiogeographical distribution of chitinozoan (“mixed layer”) marine**
46 **zooplankton biotopes for the Hirnantian glacial maximum (440Ma) are**
47 **reconstructed and compared to those from the Sandbian (460Ma): they**
48 **demonstrate a steeper latitudinal temperature gradient, and an equator-wards**
49 **shift of the Polar Front through time from 55-70°S to ~40°S. These changes are**
50 **comparable to those during Pleistocene interglacial-glacial cycles. In comparison**
51 **with the Pleistocene, we hypothesize a significant decline in mean global**
52 **temperature from the Sandbian to Hirnantian, proportional with a fall in $p\text{CO}_2$**
53 **from a modeled Sandbian level of ~8x PAL to ~5x PAL during the Hirnantian.**
54 **Our data suggest that a compression of mid-latitudinal biotopes and ecospace in**
55 **response to the developing glaciation was a likely cause of the end-Ordovician**
56 **mass extinction.**

57

58 \body

59 **Introduction**

60

61 The Hirnantian glaciation (~440 Ma) was a discrete event of a few hundred thousand
62 years (1) during the longer Early Paleozoic Ice Age (2). A Laurentide-scale
63 continental ice sheet was located in the Southern Hemisphere despite previous $p\text{CO}_2$
64 estimates ranging from 8 to 22x PAL (Pre-industrial Atmospheric Level; 3-6; for a
65 full review, see supporting online text). The Hirnantian glaciation is linked to one of
66 the major mass-extinctions in the Phanerozoic (7). New causal hypotheses for the
67 Hirnantian glaciation (2; 8) draw on a comparison with Pleistocene glacial maxima,
68 driven by orbitally-forced ice margin feedback mechanisms (9; 10), and set against a
69 background of long term $p\text{CO}_2$ decline (11). Glaciations during the late Pleistocene
70 resulted in a steepening of the latitudinal temperature gradient and a shift in the
71 position of the Polar Front from ~60° to ~40°N (12, 13). It is therefore predicted that

72 as the Hirnantian ice sheet grew and the intensity of the South Polar high pressure
73 zone increased, there would be an equatorward shift in the location of the Polar Front
74 and adjacent climate belts (14).

75

76 Stable oxygen isotope data from conodonts suggest equatorial temperatures
77 approached modern values from the Middle Ordovician (15; see ref. 16 for an
78 alternative explanation) a view supported by our previous work on plankton
79 distribution (17, 18). Proxy paleoclimate maps reconstructed for the Sandbian (~460
80 Ma), marine zooplankton (graptolite and chitinozoan) biotopes, and General
81 Circulation Models (GCMs), show tropical sea surface temperatures (SSTs) and
82 austral latitudinal temperature gradients were similar to present, and the Polar Front
83 lay between 55° to 70°S (5, 6, 17, 18; Fig. 1). These maps support GCMs in which
84 Sandbian $p\text{CO}_2$ was set at 8x PAL (5). A GCM experiment parameterized with the
85 same $p\text{CO}_2$ value, high relative sea level and a modern equator-to-pole heat transport
86 (6) returns a mean global surface temperature prediction of 15.7°C for the Sandbian.
87 Energy Balance Models (19) suggest that the elevated $p\text{CO}_2$ levels of 8x PAL could
88 have been balanced, to a large degree, by reduced solar flux from a “faint young Sun”
89 (20) to produce mean global surface temperatures that approach the modern. All this
90 is consistent with the early Late Ordovician (Sandbian) being a ‘cool’ world *sensu*
91 Royer (21).

92

93 SST maps derived from a Hirnantian GCM (assuming $p\text{CO}_2$ of 8xPAL, and a low
94 relative sea level) indicate a steepening of the temperature gradient relative to the
95 Sandbian (5; Figure 1). However, key uncertainties remain relating to the
96 parameterization of Ordovician GCMs (17, 18) and these have never been

97 independently tested. Here we present an entirely new compilation of the distribution
98 of chitinozoan zooplankton biotopes during the Hirnantian, that we use to reconstruct
99 a proxy SST-map and hence to map the position of critical climate boundaries as the
100 Earth moved into the glacial maximum of the Early Paleozoic Icehouse. We use this
101 new information to evaluate the validity of Hirnantian GCMs and estimates of
102 Hirnantian global surface temperatures and for qualitative assessments of $p\text{CO}_2$.

103

104 Our primary analysis is the same as used in our previous studies (17, 18) but here is
105 based upon an entirely new compilation of published chitinozoan species
106 presence/absence data for the glacial Hirnantian (Supplementary Figure S1). Suitable
107 collections for this interval are largely restricted to continents that fringed the
108 southern part of the Early Paleozoic Iapetus Ocean, within the southern hemisphere
109 (Figure 2).

110

111 **Results: Hirnantian chitinozoan biotope distribution**

112

113 Figure 3 shows the distribution of chitinozoan biotopes and the inferred climate belts
114 during the Hirnantian. The boundary between the Tropical and Sub-tropical
115 chitinozoan biotopes lies between 5° and 20°S ; the southern edge of the Sub-tropics is
116 at 25°S and the northern edge of the Sub-polar biotope is at 30°S . The Transitional
117 biotope lies between 25° and 30°S . The Polar Front, i.e. the northernmost extent of
118 the South Polar fauna, lies between ca. 35°S and 40°S .

119

120 Comparing the distribution of equivalent chitinozoan biotopes in the Sandbian and the
121 Hirnantian reconstructions, these key findings are reported:

122 (i) An expansion of the Polar Biotope and equator-wards shift of the Polar Front from
123 55°-70°S to ~40°S. This shift has the consequence of narrowing the Sub-Polar biotope
124 and inferred climate belt (Figure 4).

125 (ii) Within the error of our analysis there is a minimal change in the width of the
126 Tropical and Sub-tropical climate belts.

127 (iii) Species richness within biotopes appears to correlate with latitudinal extent. The
128 narrower Hirnantian Sub-polar biotope has reduced species richness (nine species
129 compared to 35 species in the Sandbian, see ref. 18), whilst the more extensive
130 Hirnantian Polar biotope has an increased species richness of 19 species compared to
131 the four species identified with certainty in Sandbian Polar faunas (18).

132 (iv) Hirnantian chitinozoan biotope distribution indicates a steeper latitudinal
133 temperature gradient than would be predicted from equivalent hypothetical plankton
134 provinces derived from the GCM with the lowest $p\text{CO}_2$ estimates (Fig. 3c, e).

135

136 **Discussion: implications for Late Ordovician global temperature and $p\text{CO}_2$ levels**

137

138 There is an ongoing debate as to how Hirnantian continental scale ice sheets could
139 exist at high $p\text{CO}_2$ levels of 8 to 22x PAL (3-6; see supporting online text). Herrmann
140 et al. (22) identified this issue and addressed it using coupled ice-sheet and
141 atmospheric GCM modeling, but concluded that initiation of glaciation was possible
142 at the lower end of these estimates. The lack of well-dated Late Ordovician direct
143 $p\text{CO}_2$ proxies (21) hampers a critical evaluation of these modeled values.
144 Furthermore, this paradox between climate state and assumed $p\text{CO}_2$ concentrations is
145 exacerbated by recent studies that conclude that Earth's climate, in the Paleozoic and
146 Pliocene, was more sensitive to atmospheric CO_2 than previously thought (23, 24).

147 Our results (point iv above) show a variance between our zooplankton maps and the
148 hypothetical distributions of plankton provinces predicted by the SSTs derived from
149 the GCM. This variation is less for the climate model with the lowest $p\text{CO}_2$ of 8x
150 PAL and implies a re-parameterization of the GCM is necessary, e.g. by using other
151 $p\text{CO}_2$ levels. Here we provide a qualitative assessment of what Hirnantian $p\text{CO}_2$ may
152 have been.

153

154 Our Late Ordovician zooplankton biotope map and climate belt reconstruction shows
155 a similar response of the Earth's climate-ocean system during the Hirnantian Glacial
156 Maximum to that reported for Pleistocene glacials. As the Hirnantian ice sheet grew,
157 the latitudinal temperature gradient steepened and the austral Polar Front shifted to
158 $\sim 40^\circ\text{S}$. The scale of shift in position of the Polar Front matches that documented
159 during Pleistocene glacial maxima and associated Heinrich Events (12, 13), and is
160 consistent with independent studies that show a coeval northward shift in the
161 Intertropical Convergence Zone (ITCZ) towards the Hirnantian (14). During
162 Pleistocene glacial maxima the boreal Polar Front moved from $\sim 60^\circ\text{N}$ to $\sim 40^\circ\text{N}$ as the
163 Laurentide ice sheet grew (12, 13) with a concomitant fall in mean global surface
164 temperature of between 3° to 5°C (based on estimated cooling between the present
165 day and the Last Glacial Maximum; 25) and a reduction of $p\text{CO}_2$ from 280 ppm to
166 180 ppm (thus at a ratio of 0.64; see ref. 11). Loi et al. (26) calculated a fall in
167 Hirnantian ice-equivalent sea-level of at least 148 m, relative to the earliest Hirnantian
168 and 222 m relative to the late Katian. These are values that are equivalent to those of
169 the total ice cover of the LGM (190-210 m; 26). We therefore hypothesize that the
170 Sandbian to Hirnantian transition resulted in similar changes in ice cover, and thus
171 ice-albedo feedback, as between Pleistocene interglacials and glacials. Combining this

172 with our results that identify similarities in amplitude of Polar Front shift, we predict a
173 similar fall in Hirnantian mean global surface temperature as during Pleistocene
174 interglacials – glacials, from 16°C pre-Hirnantian (Sandbian) to values between
175 ~13°C and ~11°C during the Hirnantian. Assuming the relationship between
176 temperature and $p\text{CO}_2$ was the same during the Ordovician and the Pleistocene (see
177 21) then we further hypothesize that $p\text{CO}_2$ fell from ~8 x PAL during the Sandbian to
178 ~5 x PAL in the Hirnantian.

179

180 **Conclusions**

181

182 Our data show that Late Ordovician SST gradients were much more similar to modern
183 oceans than previously hypothesized. Elevated $p\text{CO}_2$ (8x PAL) for the early Late
184 Ordovician appears to have balanced the reduced solar flux from a fainter Sun,
185 resulting in mean global surface temperatures that approach those of the present day.
186 Severe cooling resulted in an equatorward shift in the position of the Hirnantian
187 austral Polar Front from 55-70°S to 40°S. This is deduced from an equator-ward
188 expansion of the Polar Biotope, and is an equivalent shift to that between Pleistocene
189 interglacials and glacial maxima. We conclude that during the Hirnantian glaciation
190 there was an equatorward shift in climate belts, commensurate with a fall in mean
191 global surface temperature from ~16°C to ~13-11°C and, assuming an equivalent
192 temperature/ $p\text{CO}_2$ relationship for the Pleistocene, a fall in $p\text{CO}_2$ from 8x PAL to ~5x
193 PAL. The onset of Hirnantian glaciation was likely controlled by mechanisms and
194 feedbacks that lead to falling $p\text{CO}_2$. Significantly, our data suggest that a disruption of
195 marine habitats and a net reduction in ecospace in mid-latitude biotopes, as a
196 consequence of rapid climate change, resolves as a likely cause of the mass extinction

197 in the zooplankton at the end of the Ordovician.

198

199 **Materials and Methods**

200

201 A detailed Time Slice definition of the glacial Hirnantian (*extraordinarius* and lower
202 *persculptus* graptolite biozones, Supplementary Figure S1) and the literature sources
203 for the chitinozoan data of each site in this compilation are given in the “Materials
204 and methods” section of the supporting information. The paleolatitudes for the
205 localities are taken from the most recent paleogeographic reconstruction of Torsvik &
206 Cocks (27, updated from base maps published in 28; see supporting online text for a
207 full justification). The relatively small variance between this and earlier
208 paleogeographic reconstructions (Plate tectonic maps and “Point tracker” software by
209 C. R. Scotese, PALEOMAP Project; <http://www.scotese.com>) is used to define a 5°
210 paleogeographical error for most areas, but the position of some of the Gondwanan
211 localities varies by *ca.* 10° (Figure 3). Chitinozoan biotopes are defined using a
212 combination of Detrended Correspondence Analysis (DCA), TWINSPAN and
213 constrained seriation (17, 18; Materials and methods are available as supporting
214 material; Supplementary Figures S2-S4). The distribution of chitinozoan biotopes is
215 then compared to the hypothetical positions of modern zooplanktonic (foraminifer)
216 provinces (SST temperature boundaries from Kucera, 29), mapped onto the
217 Hirnantian paleogeography using the SST predictions from the GCMs (5; Figures 1,
218 3).

219

220 **Acknowledgements**

221 TVDB acknowledges the Research Foundation, Flanders (FWO-Vlaanderen) for
222 postdoc-project funding. JN benefited from grant 7640 of the Estonian Science
223 Foundation (ESF). We thank Alan Haywood, Yves Godd ris and Vincent Lefebvre
224 for discussion and James Baldini for constructive comments on an earlier version of
225 the text. We acknowledge the helpful comments of three anonymous referees.

226

227 **References**

- 228 1. Sutcliffe OE, Dowdeswell JA, Whittington RJ, Theron JN, Craig J (2000) Calibrating the Late
229 Ordovician glaciation and mass extinction by the eccentricity cycles of Earth's orbit. *Geology*
230 28:967-970.
- 231 2. Page AA, Zalasiewicz JA, Williams M, Popov LE (2007) Were transgressive black shales a
232 negative feedback modulating glacioeustasy in the Early Palaeozoic Icehouse? in Deep Time
233 Perspectives on Climate Change: Marrying the Signal from Computer Models and Biological
234 Proxies, eds Williams M, Haywood AM, Gregory JF, Schmidt DN (Micropalaeontological
235 Society Special Publications, Geological Society of London), pp 123-156.
- 236 3. Crowley TJ, Baum SK (1995) Reconciling Late Ordovician (440Ma) glaciation with very high
237 (14X) CO₂ levels. *J Geophys Res-Atmosph* 100:1093-1101.
- 238 4. Gibbs MT, Barron EJ, Kump LR (1997) An atmospheric pCO₂ threshold for glaciation in the Late
239 Ordovician. *Geology* 25(5):447-450.
- 240 5. Herrmann AD, Haupt BJ, Patzkowsky ME, Seidov D, Slingerland RL (2004) Response of Late
241 Ordovician paleoceanography to changes in sea level, continental drift, and atmospheric pCO₂:
242 potential causes for long-term cooling and glaciation. *Palaeogeogr Palaeoclimatol Palaeoecol*
243 210:385-401.
- 244 6. Herrmann AD, Patzkowsky ME, Pollard D (2004) The impact of paleogeography, pCO₂,
245 poleward ocean heat transport and sea level change on global cooling during the Late Ordovician.
246 *Palaeogeogr Palaeoclimatol Palaeoecol* 206: 59-74.
- 247 7. Sheehan PM (2001) The Late Ordovician Mass Extinction. *Annu Rev Earth Planet Sci* 29:331-
248 364.

- 249 8. Armstrong HA (2007) On the cause of the Ordovician glaciation. in Deep Time Perspectives on
250 Climate Change: Marrying the Signal from Computer Models and Biological Proxies, eds
251 Williams M, Haywood AM, Gregory JF, Schmidt DN (Micropalaeontological Society Special
252 Publications, Geological Society of London), pp 101-121.
- 253 9. Armstrong HA, *et al.* (2005) Origin, sequence stratigraphy and depositional environment of an
254 Upper Ordovician (Hirnantian), peri-glacial black shale, Jordan. *Palaeogeogr Palaeoclimatol*
255 *Palaeoecol* 220:273–289.
- 256 10. Clark PU, *et al.* (2009) The Last Glacial Maximum. *Science* 325:710-714.
- 257 11. Petit RJ, *et al.* (1999) Climate and atmospheric history of the past 420,000 years from the Vostok
258 ice core, Antarctica. *Nature* 399:429-436.
- 259 12. McIntyre A, Ruddiman WF, Jantzen R (1972) Southward penetrations of North-Atlantic polar
260 front - faunal and floral evidence of large-scale surface water mass movements over last 225,000
261 years. *Deep-Sea Research* 19:61-77.
- 262 13. Eynaud F, *et al.* (2009) Position of the Polar Front along the western Iberian margin during key
263 cold episodes of the last 45 ka. *Geochem Geophys Geosyst* 10:Q07U05.
- 264 14. Armstrong HA, Baldini J, Challands TJ, Gröcke DR, Owen AW (2009) Response of the Inter-
265 tropical Convergence Zone to Southern Hemisphere cooling during Upper Ordovician glaciation.
266 *Palaeogeogr Palaeoclimatol Palaeoecol* 284:227-236.
- 267 15. Trotter JA, Williams IS, Barnes CR, Lecuyer C, Nicoll RS (2008) Did cooling oceans trigger
268 Ordovician biodiversification? Evidence from conodont thermometry. *Science* 321:550-554.
- 269 16. Shields GA, Carden GA, Veizer J, Meidla T, Rong J, Li R (2003) Sr, C, and O isotope
270 geochemistry of Ordovician brachiopods: A major isotopic event around the Middle-Late
271 Ordovician transition. *Geochim Cosmochim Acta* 67:2005-2025.
- 272 17. Vandenbroucke TRA, Armstrong HA, Williams M, Zalasiewicz JA, Sabbe K (2009) Ground-
273 truthing Late Ordovician climate models using the paleobiogeography of graptolites.
274 *Paleoceanography* 24:PA4202.
- 275 18. Vandenbroucke TRA, *et al.* (in press 2010) Epipelagic chitinozoan biotopes map a steep
276 latitudinal temperature gradient for earliest Late Ordovician seas: implications for a cooling Late
277 Ordovician climate. *Palaeogeogr Palaeoclimatol Palaeoecol* doi: 10.1016/j.palaeo.2009.11.026
278 (available online).

- 279 19. Tajika E (2003) Faint young Sun and the carbon cycle: implication for the Proterozoic global
280 glaciations. *Earth Planet Sci Lett* 214:443-453.
- 281 20. Gough DO (1981) Solar interior structure and luminosity variations. *Sol Phys* 74:21-34.
- 282 21. Royer DL (2006) CO₂-forced climate thresholds during the Phanerozoic. *Geochim Cosmochim*
283 *Acta* 70:5665–5675.
- 284 22. Herrmann AD, Patzkowsky ME, Pollard D (2003) Obliquity forcing with 8-12 times preindustrial
285 levels of atmospheric pCO₂ during the Late Ordovician glaciation. *Geology* 31:485-488.
- 286 23. Breecker DO, Sharp DZ, and McFadden, LD (2010) Atmospheric CO₂ concentrations during
287 ancient greenhouse climates were similar to those predicted for A.D. 2100. *Proc Natl Acad Sci*,
288 107:576-580.
- 289 24. Lunt DJ, *et al.* Earth system sensitivity inferred from Pliocene modelling and data. *Nature Geosci*
290 3:60-64.
- 291 25. Jansen E, *et al.* Chapter 6: Palaeoclimate. in *Climate Change 2007: The Physical Science Basis*,
292 IPCC AR4, eds Solomon S, *et al.* (Cambridge Univ. Press, Cambridge and New York).
- 293 26. Loi *et al.* (in press) 2010. The Late Ordovician glacio-eustatic record from a high-latitude storm-
294 dominated shelf succession: The Bou Ingarf section (Anti-Atlas, Southern Morocco).
295 *Palaeogeogr Palaeoclimatol Palaeoecol* doi:10.1016/j.palaeo.2010.01.018 (available online)
- 296 27. Torsvik TH, Cocks LRM (2009) *BugPlates: Linking Biogeography and Palaeogeography*.
297 *Software manual* (available at <http://www.geodynamics.com>).
- 298 28. Cocks LRM, Torsvik TH (2002) Earth geography from 500 to 400 million years ago: a faunal and
299 palaeomagnetic review. *J Geol Soc London* 159:631-644.
- 300 29. Kucera M (2007) Planktonic Foraminifera as Traces of Past Oceanic Environments. in *Proxies in*
301 *Late Cenozoic Palaeoceanography*, eds Hillaire-Marcel C, De Vernal A (Developments in Marine
302 Geology volume 1, Elsevier, Amsterdam), pp 213-262.
- 303 30. Locarnini RA, Mishonov AV, Antonov JI, Boyer TP, Garcia, HE (2005) World Ocean Atlas
304 2005, Volume 1: Temperature. in NOAA Atlas NESDIS 61, ed. Levitus, S (U.S. Government
305 Printing Office, Washington, D.C.).
- 306 31. Paris F (1998) Early Palaeozoic paleobiogeography of northern Gondwana regions *Acta Univ*
307 *Carolinae-Geologica* 42:473-483.
- 308

309 **Figure Legends**

310

311 **Fig. 1.** Model predictions. (A) Latitudinal SST gradients and profiles from Sandbian
312 and Hirnantian (Caradoc and Ashgill) SST models (x8 and x15 PAL $p\text{CO}_2$, ref. 5)
313 compared with present day SST (ref. 30, central Pacific Ocean, taken from
314 <http://www.noaa.gov>). Modern day planktonic foraminifer provinces in terms of SST
315 (29). (B) Using SST simulations of Herrmann *et al.* (5) at x8 (High Sea Level/Low
316 Sea Level) and x15 PAL $p\text{CO}_2$ we estimate the position of these zooplankton
317 provinces/belts and their boundaries during the Hirnantian, for different $p\text{CO}_2$
318 scenarios.

319

320 **Fig. 2.** Paleogeographical reconstruction (27). The shading represent TWINSPAN
321 clusters, i.e. Polar (black), Tropical (white) and Sub-Polar to Sub-tropical localities
322 (grey; Materials and methods are available as supporting material). *We do not follow
323 this reconstruction for the Prague Basin on the wandering Perunica ‘microcontinent’,
324 which is shown to have been at higher paleolatitudes (31).

325

326 **Fig. 3.** Plankton maps. (A) Map of modern planktonic foraminifer provinces. (B, C,
327 D) Hypothetical plankton models based on GCMs parameterized as indicated. (E)
328 Comparing inferred chitinozoan biotopes with the hypothetical plankton models
329 allows us to identify Hirnantian Tropical to Polar chitinozoan biotopes, with key
330 boundaries at ~20, 25, 30, 40°S. Hence we can map oceanic climate belts during the
331 major glaciation of the Early Paleozoic and compare these to the pre-glacial Sandbian
332 climate belts (see Fig. 4). The chitinozoan biotopes and their inferred climate belts are
333 most similar to the patterns for the hypothetical planktonic provinces for a SST-model

334 at x8 PAL $p\text{CO}_2$ and low relative sea levels, but nevertheless indicate an even steeper
335 faunal and hence latitudinal temperature gradient than the model. The dots represent
336 localities and the error bars reflects variance with regard to PALEOMAP
337 reconstructions (<http://www.scotese.com>) with a minimum of 5° of latitude.

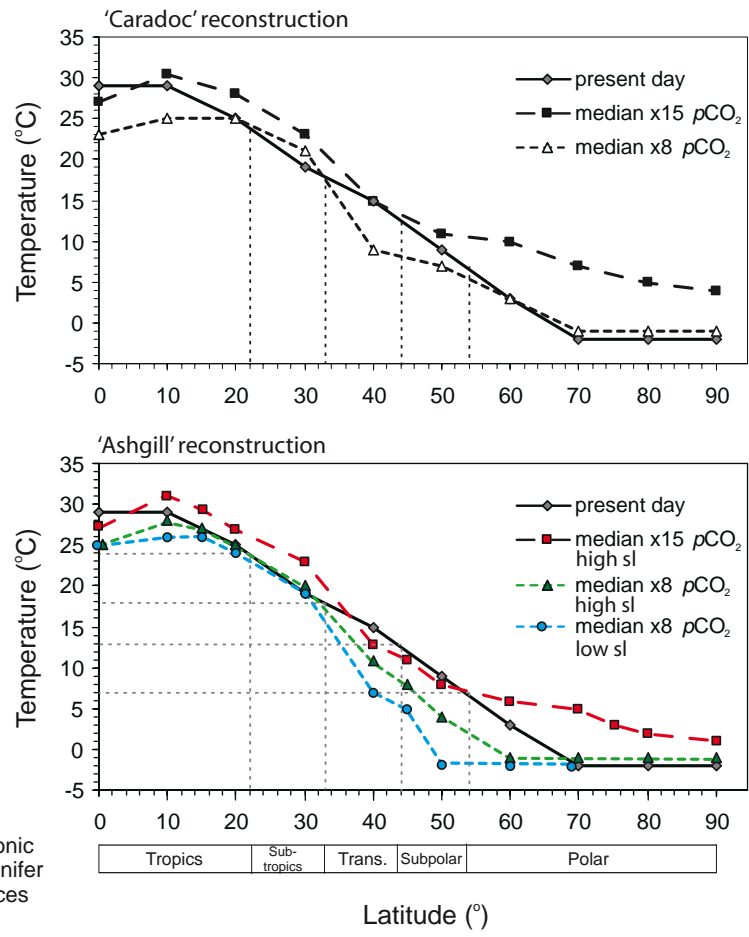
338

339 **Fig. 4.** Late Ordovician Polar Front migration. Time line showing a Katian (2) start of
340 Late Ordovician cooling and a revised view with an earlier onset (15). Our Sandbian
341 data (17, 18) support the latter. The map view compares Sandbian and Hirnantian
342 chitinozoan biotopes; these maps demonstrate an equatorward shift in the position of
343 the Polar Front from $55^\circ\text{-}70^\circ\text{S}$ to likely 40°S , which involves an equatorward
344 incursion of Polar water and a compression of the Sub-polar belt and fauna
345 (diversity). The sub-tropical belt moves slightly northwards. The shift of the Polar
346 Front maps onto well-known patterns of late Cenozoic glacial-interglacial Polar Front
347 migration.

348

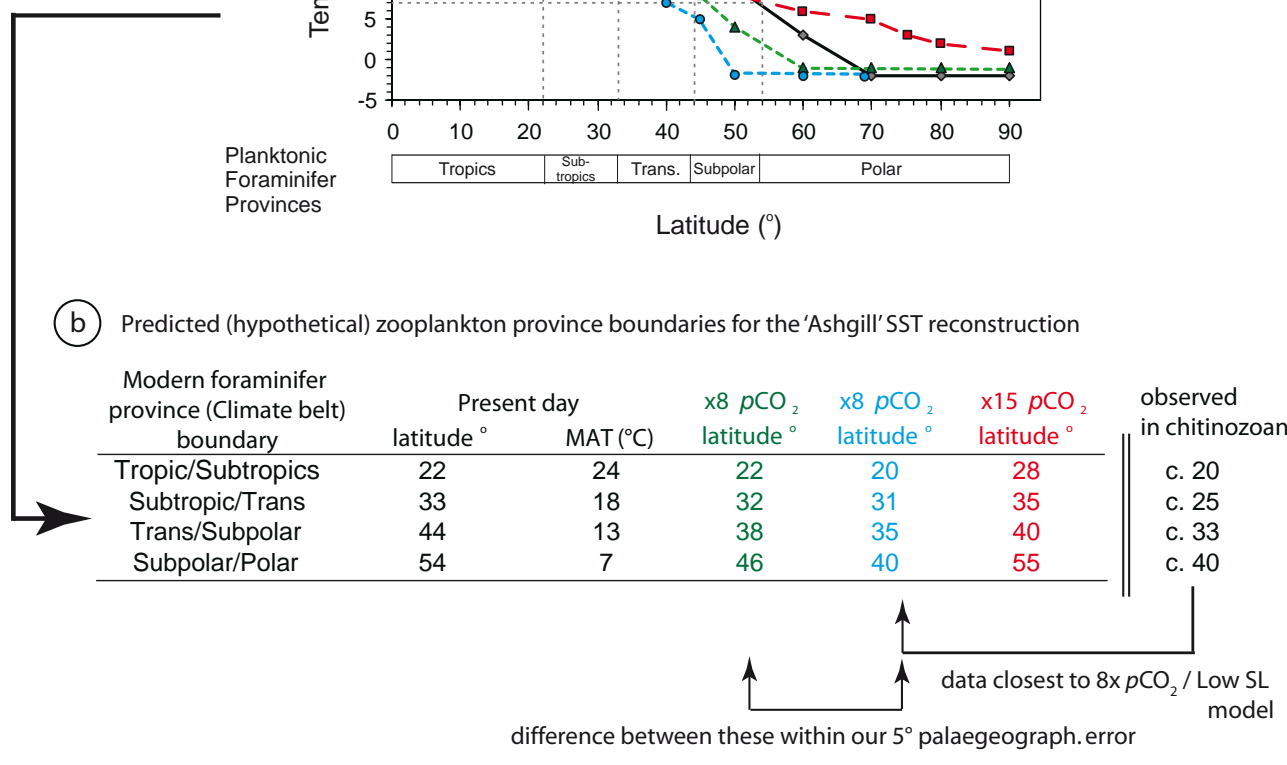
Figure 1

(a) Predicted SST gradients (Herrmann *et al.* - ref 5) versus modern



(b) Predicted (hypothetical) zooplankton province boundaries for the 'Ashgill' SST reconstruction

Modern foraminifer province (Climate belt) boundary	Present day		x8 pCO ₂	x8 pCO ₂	x15 pCO ₂	observed in chitinozoans
	latitude °	MAT (°C)	latitude °	latitude °	latitude °	
Tropic/Subtropics	22	24	22	20	28	c. 20
Subtropic/Trans	33	18	32	31	35	c. 25
Trans/Subpolar	44	13	38	35	40	c. 33
Subpolar/Polar	54	7	46	40	55	c. 40



data closest to 8x pCO₂ / Low SL model

difference between these within our 5° palaeogeograph.error

Figure 2

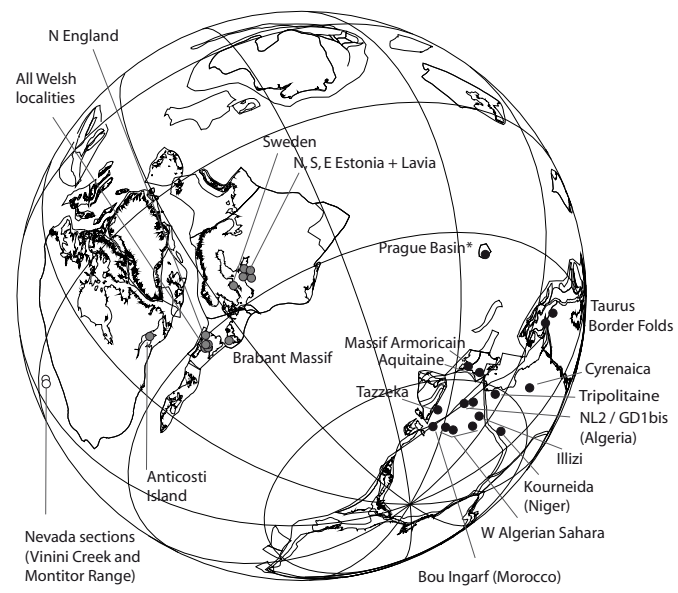


Figure 3

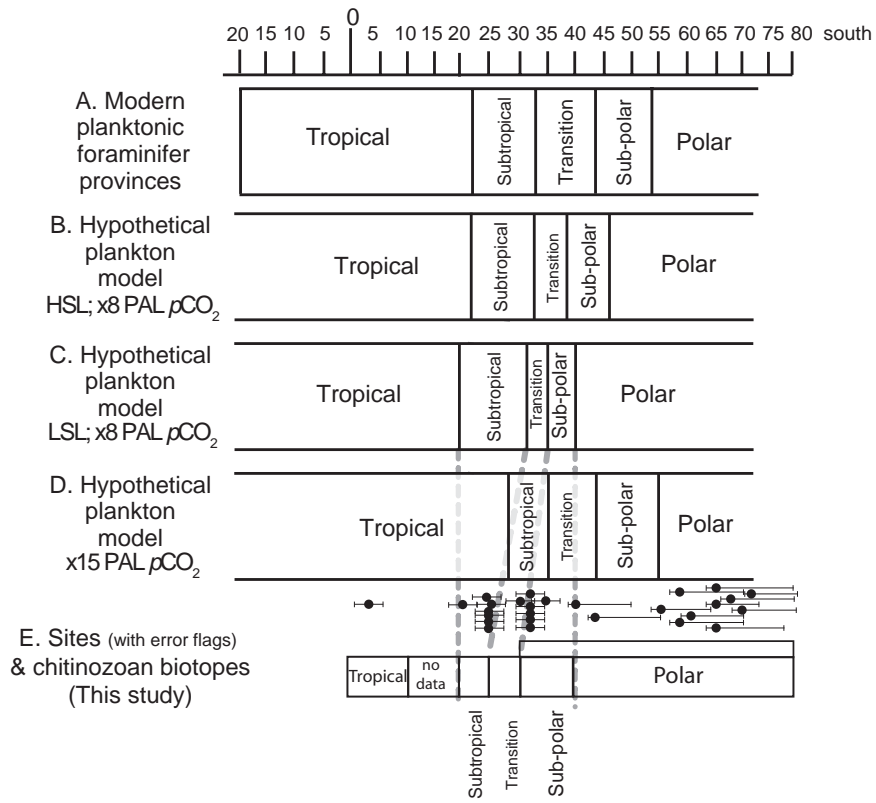
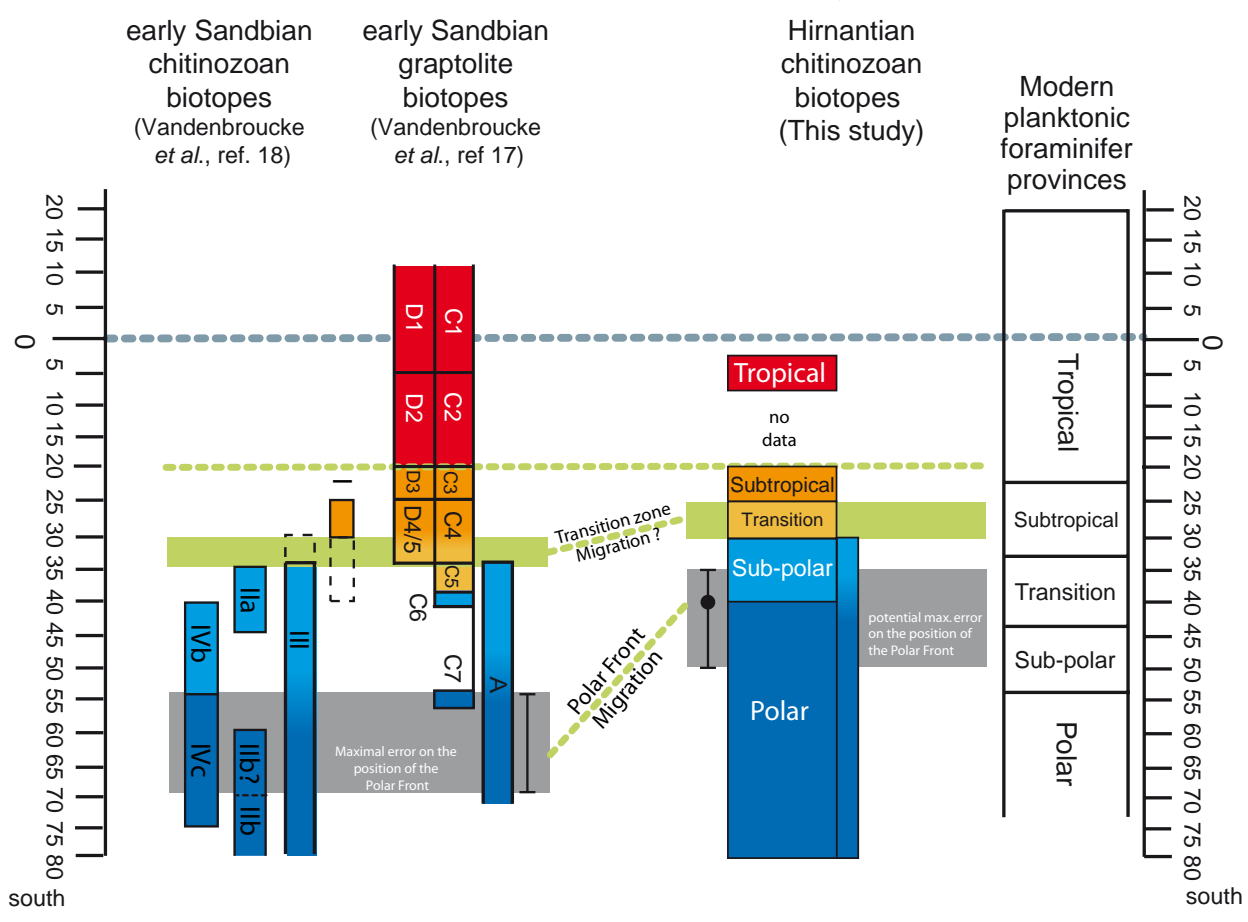
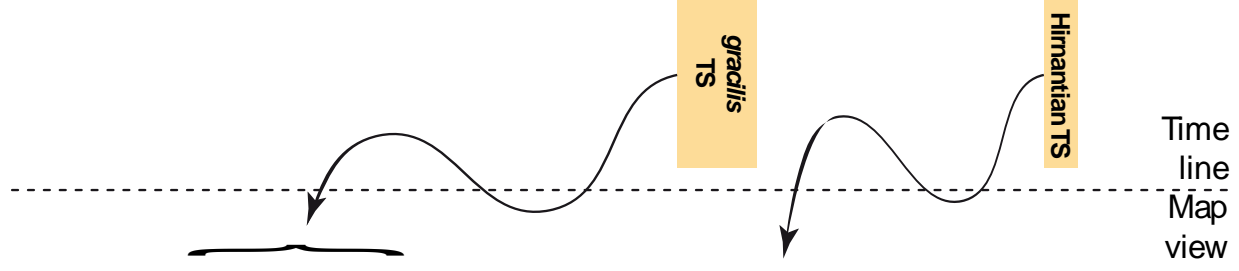


Figure 4

LOWER ORDOVICIAN		MIDDLE ORDOVICIAN		UPPER ORDOVICIAN			GLOBAL SERIES & STAGES
TREMADOCIAN	FLOIAN	DAP.	DARRIWILIAN	SANDBIAN	KATIAN	Hi.	BRITISH SERIES
Tremadoc	Arenig		Llanvirn	Caradoc		Ashgill	
Greenhouse				icehouse			climate state classic view
Greenhouse ?				icehouse			climate state revised view



early Sandbian chitinozoan biotopes (Vandenbroucke *et al.*, ref. 18)

early Sandbian graptolite biotopes (Vandenbroucke *et al.*, ref 17)

Hirnantian chitinozoan biotopes (This study)

Modern planktonic foraminifer provinces

Time line
Map view

20 15 10 5 0
5 10 15 20 25 30 35 40 45 50 55 60 65 70 75 80
south

20 15 10 5 0
5 10 15 20 25 30 35 40 45 50 55 60 65 70 75 80
south